"EVALUATION OF OUTER RACE TILT AND LUBRICATION ON BALL WEAR AND SSME BEARING LIFE REDUCTIONS"
(Contract NAS8-34908, Task No. 109)

to

ATIONAL AERONAUTICS AND SPACE ADMINISTRATION
GEORGE C. MARSHALL SPACE FLIGHT CENTER
MARSHALL SPACE FLIGHT CENTER, ALABAMA 35812

July 7, 1983

FINAL REPORT

on

"EVALUATION OF OUTER RACE TILT AND LUBRICATION ON BALL WEAR AND SSME BEARING LIFE REDUCTIONS"

(Contract NAS8-34908, Task No. 109)

to

NATIONAL AERONAUTICS AND SPACE ADMINISTRATION
GEORGE C. MARSHALL SPACE FLIGHT CENTER
MARSHALL SPACE FLIGHT CENTER, ALABAMA 35812

July 7, 1983

by

J. W. Kannel, T. L. Merriman,
R. D. Stockwell, and K. F. Dufrane

BATTELLE
Columbus Laboratories
505 King Avenue
Columbus, Ohio 43201

ABSTRACT

The objective of this task has been to evaluate several aspects of the SSME bearing operation. Analyses were conducted to evaluate the possibility of EHD lubrication with a cryogenic fluid. Films as thick as .61μ (24 μin.) were predicted with one theory which may be thick enough to provide hydrodynamic support. However, the film formation is heavily dependent on good surface finish and a low (150 K (<270 R)) bulk bearing temperature. In addition, bearing dynamic analyses were conducted to determine if the radial stiffness of a bearing is dependent on bearing misalignment. Finally, numerous 4-ball tests were conducted at several environmental conditions from an LN_2 bath to 426 C (800 F) in air. The tests involved evaluation of surface coatings and ball materials. Severe wear and high friction were measured for all ball materials except when the balls had surface lubricant coatings.

CONCLUSIONS

The research for this task was directed at several aspects of the SSME LOX pump bearing performance. As a result of this task, the following conclusions can be made.

1. Partial elastohydrodynamic (EHD) lubrication of the SSME bearings may occur with LOX as the lubricant. However, the predicted lubricant films are very thin and dependent on bulk bearing temperature. In addition, the lubrication is contingent on the LOX wetting the bearing surface. Finally, if the bulk bearing temperature exceeds 270 R, EHD formation is impossible because of vaporization of the LOX.

2. Experiments are needed (and planned for Task 110) to evaluate cryogenic EHD lubrication. These experiments should demonstrate if EHD lubrication is (or is not) feasible in an SSME bearing.

3. The radial stiffness in an SSME bearing is not significantly dependent on bearing misalignment nor does stiffness vary with radial position around the bearing.

4. Ball race slippage with a magnitude of .76-1.5 m/sec (30 - 60 in./sec) will occur in the SSME bearing.

5. In the absence of surface coatings, ball wear and friction in a bearing will be severe. The bearing material 440C will incur somewhat greater wear than BG-42 but significantly less wear than Star-J.

6. With surface coatings, wear and friction can be greatly reduced for the duration of the coating. Coatings lives as long as 45 minutes were measured with a BG-42 ball in the 4-ball tests which would be as much as 135 minutes in an engine under near ideal conditions (at room temperature). However, the maximum coating life at cryogenic temperature was 8.5 minutes (25.5 minutes in a bearing).

7. At elevated temperatures 204 - 427 C (400 to 800 F) friction is reduced. However, ball wear is still a major problem.

NEEDED FURTHER RESEARCH

Based on the studies conducted in this task, the following general observations about SSME bearing lubrication can be made. The key to SSME bearing performance is the solid surface films on the balls and races. These films must be precoated, or preferably transfered, from cage to balls to races. Cryogenic EHD lubrication may help but forming films of useful thicknesses may not be realistic. Likewise, better bearing materials may be found to improve the bearing life, but it is probable that their improvements will be small.

Much more research is needed to define conditions which promote transfer film lubrication. Since PTFE has been found to be a good transfer film lubricant, experiments should be centered around this material. The effect of ball material, surface finish, and surface pretreatment and coatings on transfer film rate and film durability should be evaluated. Cage designs and material matrix configurations should be evaluated to optimize the lubrication process. In our opinion, transfer film optimization is the key to SSME bearing performance.

"EVALUATION OF OUTER RACE TILT AND LUBRICATION ON BALL WEAR AND SSME BEARING LIFE REDUCTIONS"

by

J. W. Kannel, T. L. Merriman,
R. D. Stockwell, and K. F. Dufrane

INTRODUCTION

The impressive success of the space shuttle has clearly demonstrated the feasibility of the system and has undoubtedly fostered a new trend in space craft technology. It is imperative, then, that efforts be expanded to develop the technology required for maintenance free reusable systems for at least the target of 7.5 hours. In this regard, the bearings in the space shuttle main engine (SSME) continue to represent a long term problem area. The bearings must operate at very high DN* values (1.7×10^6) under poor lubrication conditions. The bearings lubrication must be derived from cyrogenic hydrogen or oxygen and/or from transfer from the cage material (PTFE).

Battelle has been assisting NASA in bearing development of the SSME bearings through a task order arrangement. The current task was scheduled for several activities including metallurgical analyses, theortical analyses of cryogenic lubrication, analyses of misalignment effects on bearing stiffness, evaluation of ball wear at ambient temperatures for various materials and coatings, and evaluation of ball wear at extreme temperatures (cryogenic and high).

This report summarizes the work on the various activities mentioned above. It should be noted that since no bearings were available from the sponsor, no metallurgical analyses were conducted. However, considerable success was achieved in the other areas of the task. The report is divided

*DN = Bore diameter (mm) x rpm

into two sections as follows:

1. Theoretical studies of ball loading and cryogenic lubrication, and

2. Experimental studies of ball wear.

THEORETICAL STUDIES

Hydrodynamic Film Thickness

The objective of this analyses has been to evaluate if the SSME LOX pump bearings might be hydrodynamically lubricated with liquid oxygen. In more standard bearing applications, a hydrodynamic film is found as a result of the lubricant drawn between the balls and races. This type of lubrication is known as elastohydrodynamics (EHD) as a result of the elastic deflection of the balls in conjunction with the hydrodynamics of the lubricant. Even with conventional hydrocarbon lubricants, EHD films are only on the order of a few millionths of an inch. However, since bearing ball and race surfaces are extremely smooth (on the order of .12μ (5 μin.) c.l.a.),such thin films are sufficient to protect the bearings elements from metallic contact.

There are three difficulties in achieving good EHD films with cryogenic fluids.

1. The base viscosity is lower by an order of magnitude than conventional lubricants.

2. The viscosity of cryogenic fluids probably does not increase with pressure as do conventional lubricants.

3. The cryogenic fluids may vaporize due to bearing heating.

Basic Film Thickness Equations

There are two bearing (EHD) film thickness theories for conditions where viscosity does not vary with pressure. One is an equation developed by H. S. Cheng[1]* which can be written:

$$\frac{h_m}{R} = 2.78\ \bar{p}_H^{1/2}\ \bar{U}^{5/8} \quad , \tag{1}$$

where

h_m is film thickness in the contact zone (see Figure 1)

$\bar{p}_H = p_H/E_D$

p_H is maximum Hertz contact pressure

$$\frac{1}{E_D} = 1/2\left(\frac{1 - \nu_1^2}{E_1} + \frac{1 - \nu_1^2}{E_1}\right)$$

E_1, E_2 are the moduli of the bearing balls and races

ν_1, ν_2 are Poisson ratios

$$\frac{1}{R} = \frac{1}{R_1} + \frac{1}{R_2}$$

R_1, R_2 are the rolling radii of the balls and races

$$\bar{U} = \frac{\mu_o\ (u_1 + u_2)}{2E_D\ R}$$

μ_o is base viscosity

u_1, u_2 are the rolling velocities of the balls and races.

The second equation is one developed at Battelle[2], which can be written in general terms as

$$\frac{h_m}{R} = 1.65\left(\frac{\mu_o}{\bar{U}\ p_H}\int_o^{p_e}\frac{dp}{\mu}\right)^{-8/14}\left(\frac{E_D}{p_H}\right)^{10/11} \quad . \tag{2}$$

*References are listed on page .

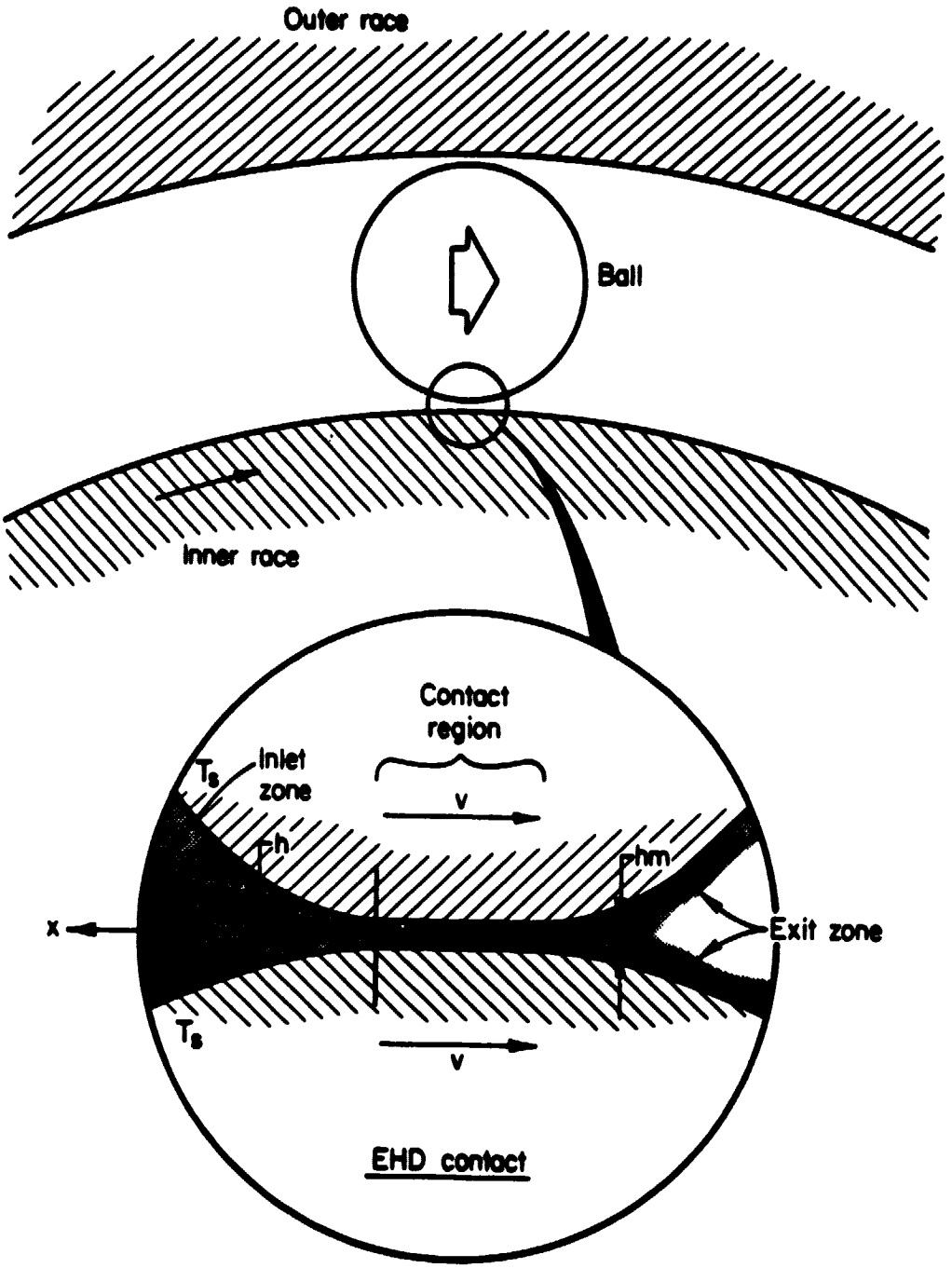

FIGURE 1. COORDINATE SYSTEM FOR BALL RACE (EHD) FILM THICKNESS EVALUATIONS

If μ (viscosity) is a constant, then Equation (2) can be written

$$\frac{h}{R} = 1.65 \left(\frac{\bar{u}}{n}\right)^{8/11} \left(\frac{E_D}{p_H}\right)^{10/11} , \qquad (3)$$

where n is ratio of the pressure at the front edge of the contact region to the Hertz maximum pressure.

If the lubricant were to vaporize in the film formation process, then μ would not be a constant but rather would drop to a very low value at the point of vaporization. If this value of μ is set equal to zero in Equation (2), then

$$\frac{hm}{R} = 0 \quad \text{regardless of when vaporization occurs.} \qquad (4)$$

In general, then, Equation (1) or (3) can be used to evaluate EHD film thickness provided that the viscosity is continuous. If vaporization occurs, then no film exists.

Vaporization Conditions

The conditions which promote the vaporization of the cryogenic fluids are discussed in Appendix A. For liquid oxygen, Equation (A-11) shows the critical temperature and Equation (A-13) shows the heat of vaporization. Essentially, if the temperature exceeds 156 K (280 R), flash vaporization will occur. Temperatures below this level cause vaporization provided that sufficient heat is available.

Equation (A-17) is an expression for the total heat applied to an element of the cryogenic fluid as it enters the conjunction region between ball and race. (See Figure A-2.) The average temperature is given by Equation (A-20).

Example of Cryogenic Film Thickness

A computer model was developed to evaluate the temperature and total heat developed as a cryogenic fluid approaches the contact region between the ball and races. To check the film thickness computations

the predictions were compared with films measured using water as a lubricant. The film thickness measurements were achieved using an X-ray technique in conjunction with a twin disk (.076 m (3 in.) diameter) apparatus. Water has a viscosity of the same order of magnitude as liquid oxygen and, in addition has a near zero pressure viscosity exponent. The results of this comparison are shown in Table 1 below. In general, the Battelle theory seems to predict films which more closely agree with experiments than does the Cheng predictions.

TABLE 1. COMPARISON OF MEASURED AND PREDICTED EHD FILM THICKNESS (WATER)

Pressure, MPa (ksi)	Speed, m/s (ips)	Film Thickness, μm (μin.)		
		Measurement	H_B(Battelle)	H_C(Cheng)
152(22)	18.3(721)	2.0(79)	.99(39)	.028(1.1)
220(32)	18.3(721)	.56(22)	.61(24)	.024(.96)

Typical film thickness and thermodynamic predictions for the SSME LOX pump bearing are given in Table 2. It can be seen that very thin films are predicted for cryogenic fluid lubrication although the films predicted using the Battelle model tend to be thicker than predicted by the Cheng model. If the bearing surface could be polished to achieve a very smooth surface finish, it is possible that cryogenic fluids could yield some hydrodynamic support.

A second area of interest in Table 2 pertains to the heat of vaporization. It appears that the cryogenic fluid will not vaporize provided that the surface temperature of the bearing is below about 150 K (270 R). This temperature is probably the average ball and race temperature, or more generally, the bulk temperature of the bearing. In conclusion then, if the bulk bearing temperature is less than, say, 150 K (270 F), hydrodynamic lubrication is possible. However, experiments with actual cryogenic fluids are needed to evaluate this hypothesis. Experiments of this nature will be described in the report on Task 110 of the project.

TABLE 2. PREDICTION OF FILM FORMING CAPABILITY OF CRYOGENIC FLUIDS IN SSME LOX PUMP BEARING

Contact Stress GPa(KSI)	Speed rpm	Surface Temperature °K(°R)	Film Thickness μm(μin) HB	Film Thickness μm(μin) HC	Tap °K(°R)	Tvp °K(°R)	Q_{TOT} $\frac{in\text{-}lbs}{in^3}$	Hvp $\frac{in\text{-}lbs}{in^3}$
1.37(200)	30000	55(100)	.61(24.0)	03(1.4)	64(114)	155(280)	$.09 \times 10^5$	$.18 \times 10^5$
2.10(300)	30000	55(100)	.43(17.0)	03(1.2)	65(116)	155(280)	$.15 \times 10^5$	$.26 \times 10^5$
1.37(200)	30000	111(200)	.17(6.5)	01(.45)	112(202)	155(280)	$.1 \times 10^5$	$.17 \times 10^5$
2.10(300)	30000	111(200)	.12(4.6)	01(.4)	112(202)	155(280)	$.12 \times 10^5$	$.16 \times 10^5$
1.37(200)	30000	139(250)	.13(5.1)	01(.4)	140(252)	155(280)	$.10 \times 10^5$	$.16 \times 10^5$
2.10(300)	30000	139(250)	.10(3.6)	01(.3)	140(252)	155(280)	$.11 \times 10^5$	$.15 \times 10^5$

Tap = Average temperature at edge of contact

Tvp = Temperature required to vaporize LOX at edge pressure condition

Q_{TOT} = Total (average) heat in fluid

Hvp = Heat of vaporization at temperature condition

Effect of Misalignment on Bearing Stiffness

A second aspect of the theoretical analysis has been to evaluate the effect of serious misalignment on bearing radial stiffness. These calculations involved the use of the Battelle bearing dynamics computer-model BASDAP. BASDAP is the model which can be used to evaluate ball-race force and internal bearing deflections. In the current task, BASDAP was used to predict radial deflections of the bearing at different angular locations for given radial loads. The results of these computations are summarized in Table 3. For this table

δ = radial deflection due to both effects of radial loading and misalignment.

δ_L = radial deflection due to radial loading only, the effect of misalignment was subtracted out in the follow manner:

$\delta_L = \delta_{400 \text{ pound radial load}} - \delta_{1 \text{ pound radial load}}$,

(for a given misalignment and phase angle).

The misalignment causes the shaft to shift downwards, causing the deflections listed under the 1 pound loads. One pound is taken to be essentially equal to zero load and is necessary in order to get the computer model to run.

With the effect of misalignment subtracted out, the deflections δ_L (therefore bearing stiffness) are seen to be approximately the same at all phase angles, for the 400-pound load entries. For these cases, δ_L varies from .174 to .156 x 10^{-3} inch which is an extremely slight variation.

Maximum cage load is calculated for those cases where the ball excursion exceeded the ball-pocket diametral clearance (.024 inch for the SSME LOX pump bearing). Under severe misalignment, very high cage loads can occur, which, under repeated operation, would damage the bearing-cage.

TABLE 3. EFFECT OF MISALIGNMENT ON RADIAL DEFLECTION OF SSME LOX PUMP BEARING

Radial Load, N(lb)	Phase Angle, degree	Misalignment, degree	δ_L* (10^{-3} in)	δ* (10^{-3} in)	Ball Excursion, inch	Maximum Cage Load, N(lb)	Temperature Rise at ball-race contact	
							Outer K(°R)	Inner K(°R)
4.448(1)	0	.0057	-	-.0737	.0039	-	10(17.7)	74(132.7)
4.448(1)	166.2	.0057	-	.0724	.0052	-	10(17.5)	72(128.5)
4.448(1)	0	.0372	-	-.481	.0246	200(45.0)	10(17.8)	78(140.5)
4.448(1)	55.4	.0372	-	-.273	.0928	298(67.1)	13(22.8)	86(154.2)
4.448(1)	110.8	.0372	-	.169	.1555	311(70.1)	13(22.9)	86(154.3)
4.448(1)	166.2	.0372	-	.468	.0341	222(49.7)	9(16.3)	76(136.8)
1783(400)	0	.0057	.174	.0998	.0326	236(53.4)	10(17.7)	74(132.7
1783(400)	166.2	.0057	.164	.236	.0234	-	10(17.5)	72(128.5)
1783(400)	0	.0372	.165	-.316	.0509	240(54.2)	10(17.8)	79(143.3)
1783(400)	55.4	.0372	.156	-.117	.1001	307(68.6)	13(22.8)	86(154.2)
1783(400)	110.8	.0372	.168	.337	.1574	316(71.4)	13(23.5)	84(151.6)
1783(400)	166.2	.0372	.163	.631	.2314	245(54.6)	10(18.1)	73(130.7)

* To convert to m, multiply by .025.

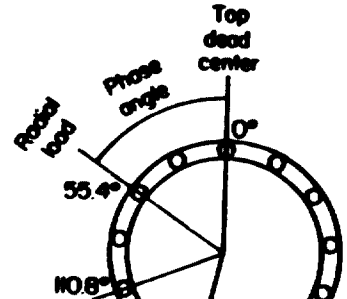

Evaluation of Ball Race Slippage

, third aspect of the analysis has been to evaluate ball-race slip in the SSME bearings. In a liquid lubricated bearing, such slip is normally of only secondary importance. However, in a bearing where significant metal to metal contact can occur, such as a bearing lubricated with only a cryogenic fluid, ball race slip can be a major source of bearing distress. The BASDAP computer program was modified to predict and print any gross ball-race slip.

In the BASDAP computations, the balls are assumed to be in an equilibrium torque condition. That is, the spin torque at the ball-outer race contact is assumed to be the same as the spin torque at the ball-inner race contact. This equilibrium condition is assumed for all three axes of ball rotation. In this regard, the BASDAP model is somewhat different from the A. B. Jones model which uses a race-control hypothesis. This hypothesis requires that the ball contacts producing the largest torque controls the ball spin and that the ball spins freely on the other race. The BASDAP model should be the more realistic representation of a bearing of the two models. Based on calculations using the BASDAP model, it has been concluded that ball slip is due only to the ball spin about its point of contact at the inner or outer races. That is, no gross slippage of the ball was predicted by the model.

The average ball slippage in a bearing can be approximated by the equation

$$V_{slip} \approx \frac{\omega_s a}{2} \quad , \tag{5}$$

where ω_s is the ball spin rate, and a is the half length of contact. A typical value for a is.001 m (.062 inch) and for ω_s is 10^4 rev/min (10^3 rad/sec At 30,000 rpm with a 8896N (2000 pound) axial load, then the average slippage in an SSME bearing is

$$V_{slip} = .81 \text{ m/sec } (32 \text{ in./sec}) \quad . \tag{6}$$

This slippage will increase linearly with speed and only slightly with load. At 35584N (8000 pound) axial load

$$V_{slip} \approx 1.6 \text{ m/sec } (64 \text{ in./sec}) \quad . \tag{7}$$

EXPERIMENTAL STUDIES

Four-Ball Test Apparatus

The objective of the current experiments has been to evaluate the wear of SSME LOX pump bearing balls under realistic load, slip, and temperature conditions. The experiments were conducted with a 4-ball wear tester (see Figures 2 and 3). This apparatus has been used for numerous types of wear testing under pure-sliding contacts.

Several types of tests were scheduled for the project as summarized in Table 4.

TABLE 4. MATRIX FOR 4-BALL TESTS

Ball Materials	Coating Materials*	Environment
52100	MoS_2 - 1/2 μm thick	Dry - Room Temperature
440C	MoS_2 - 1-1/2 μm thick	LN_2
BG-42		Hot 204 - 426 C (400 - 800 F)
Star-J		

Several modifications were made to the apparatus to permit experiments in a cryogenic fluid (LN_2), as well as at high temperatures. Essentially, the apparatus consists of a long shaft which extends from a drill press. The shaft is attached to the upper ball of the test configuration. The lower three balls are attached to a mandrel which is mounted in angular contact bearings. A load cell constrains the lower balls and is used to monitor torque.

The load and speed conditions for the tests were selected to evaluate the conditions in an actual SSME bearing. One major difference in the wear mechanism in the 4-ball configuration, in comparison with the bearing, is the exposed wear surface. For the 4-ball apparatus, wear occurs over a local track, whereas for the bearing, wear can occur over the entire

*Coatings were prepared (under contract) by Holman plating. The 1/2 μm coatings were sputtered and the 1-1/2 μm coatings were co-sputtered with nickel.

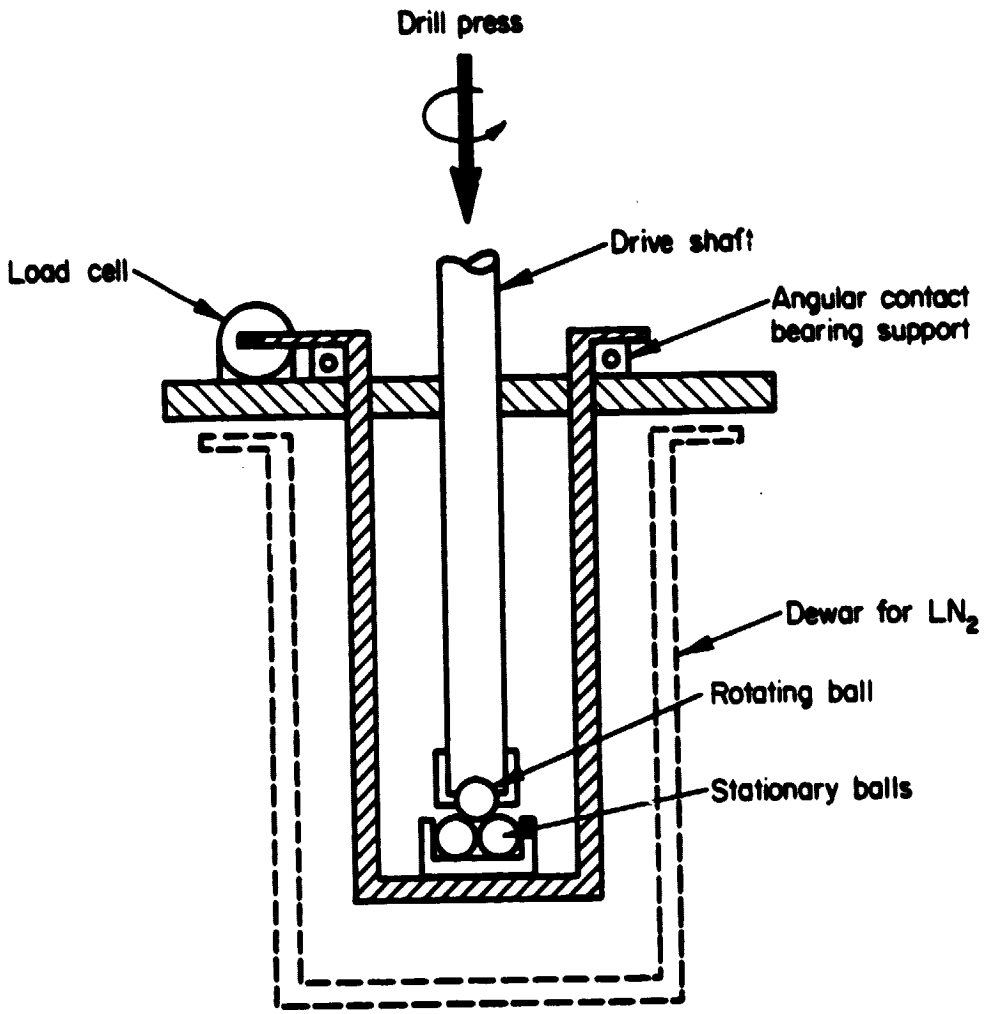

FIGURE 2. SCHEMATIC DRAWING OF FOUR BALL FIXTURE FOR WEAR EXPERIMENTS

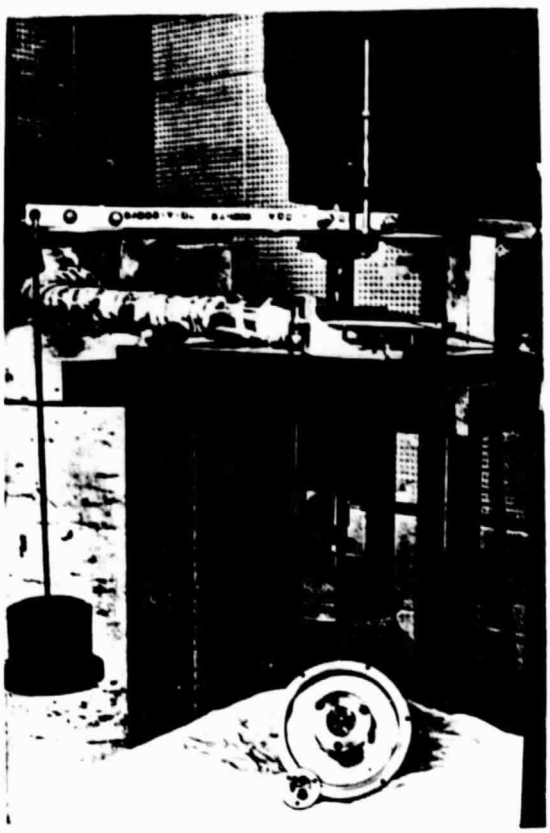

FIGURE 3. PHOTOGRAPH OF MODIFIED 4-BALL CONFIGURATION CAPABLE OF OPERATING AT CRYOGENIC TEMPERATURES

ball surface. To evaluate the 4-ball wear condition, consider the sketch in Figure 4.

The load on any ball can be expressed

$$L_B = W/3 \sin 60 \quad . \tag{8}$$

The area of the path on the rotating ball can be expressed

$$A_{4\text{-ball}} = \frac{2\pi r_c}{3} (2a) \quad , \tag{9}$$

where a is the radius of the Hertz contact. The factor of 3 in the demoninator is the result of 3 contacts (balls) per revolution of the center ball.

The effective wear path area for the ball in the bearing is the surface or

$$A_{brg} = 4\pi r_B^2 \quad . \tag{10}$$

For comparison of the 4-ball configuration to the bearing, it is convenient to define a hypothetical wear-depth-rate term as follows

$$\dot{\delta} = \frac{C_w P V_{slip}}{A_{eff}} \quad , \tag{11}$$

where C_w is a constant, P is the local load, V_{slip} is slip velocity, A_{eff} is the area of the wear surface, δ is the depth of the wear track and $\dot{\delta}$ is the time rate of change of δ. Figure 5 shows the ratio of wear depth for the 4-ball rig in comparison to an SSME bearing (30,000 rpm @8896N (2000 pound) axial load, as discussed in the previous section) as a function of applied load W. The .012 m (.5 inch) diameter balls were assumed for both the 4-ball tester and the bearing.

A load of 165N (37 pounds) was used as the test load. This load should accelerate ball wear by about a factor of three over bearing wear and further it should produce a Hertz contact stress of about 2.4 GPa (350,000 psi) which is similar to the stresses in a bearing under a 8896N (2000 pound) axial load.

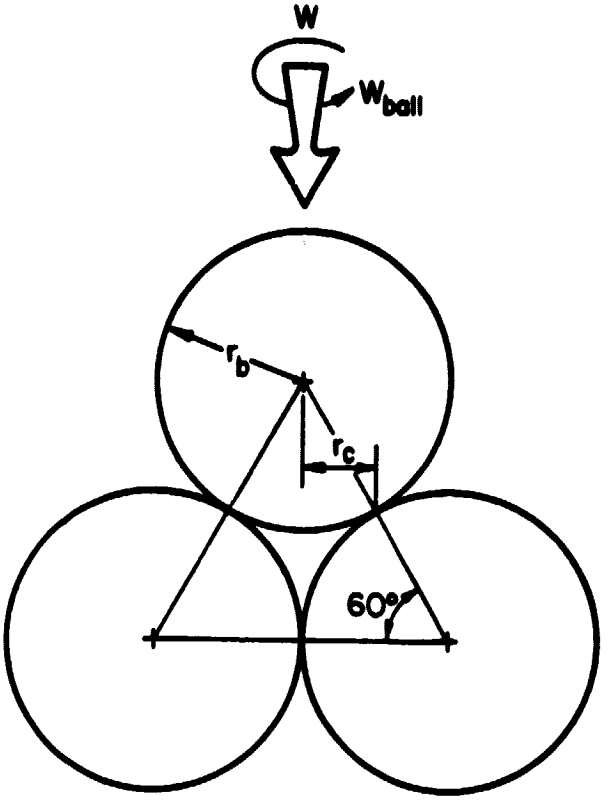

FIGURE 4. NOMENCLATURE FOR 4-BALL CONFIGURATION

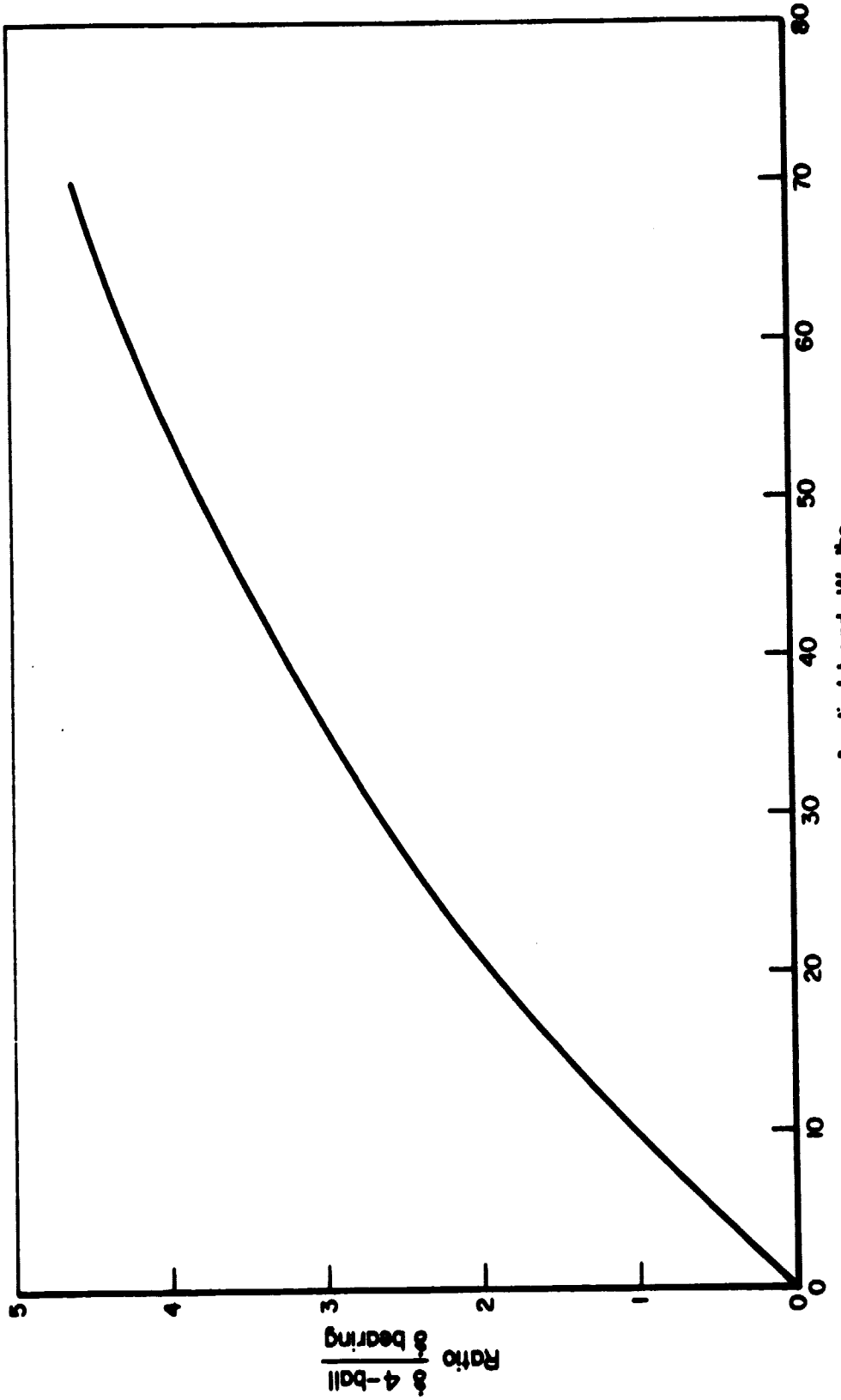

FIGURE 5. HYPOTHETICAL WEAR RATE IN 4-BALL RIG VERSUS ACTUAL SSME BEARING

Wear Tests at Room Temperature

The initial experiments involved measuring wear as a function of time on a 440C and an AISI 52100 ball-specimen. For the 4-ball tests, the critical wear measurement is the effective wear scar diameter. The "wear scar" is taken as the average of the largest and smallest diameter of the worn surface on the three stationary balls. That is, each point represents the average of 6 measurements. Graphs showing the growth of the wear scar are shown in Figures 6 and 7 along with computed wear volume.* These tests clearly indicate that the volume wear rate is essentially constant even though the growth of the wear scar diminishes with time during the period.

The next set of experiments involved wear studies at room temperature with various material combinations. The results are summarized in Table 5. For the uncoated balls, the width of the wear scar varied from 1.64 mm (.0646 in.) to 3.58 mm (.141 in.) and the friction coefficient was on the order of .39 to .57. When the balls were coated with M_oS_2, the wear scar size was reduced to as low as 1.44 mm (.057 in.).

One very important feature of the coated ball experiments was that a very low coefficient of friction (<.03) occurred in the initial stage of operation. At some point in time, the friction jumped to the higher level presumably due to the destruction of the surface coating. For the BG-42 ball, the coating lasted as long as 45 minutes and for the Star-J ball, the coatings endured for 25 minutes.

Test at Cryogenic Temperature

Since the SSME LOX pump bearings must operate in a cryogenic environment, there is a question about the validity of 4-ball tests at room temperature. To evaluate this problem, 4-ball tests in LN_2 were scheduled as a part of the project. For these experiments, a Dewar is

*Wear volume is computed as twice the volume of spherical segment defined by the wear scar circle.

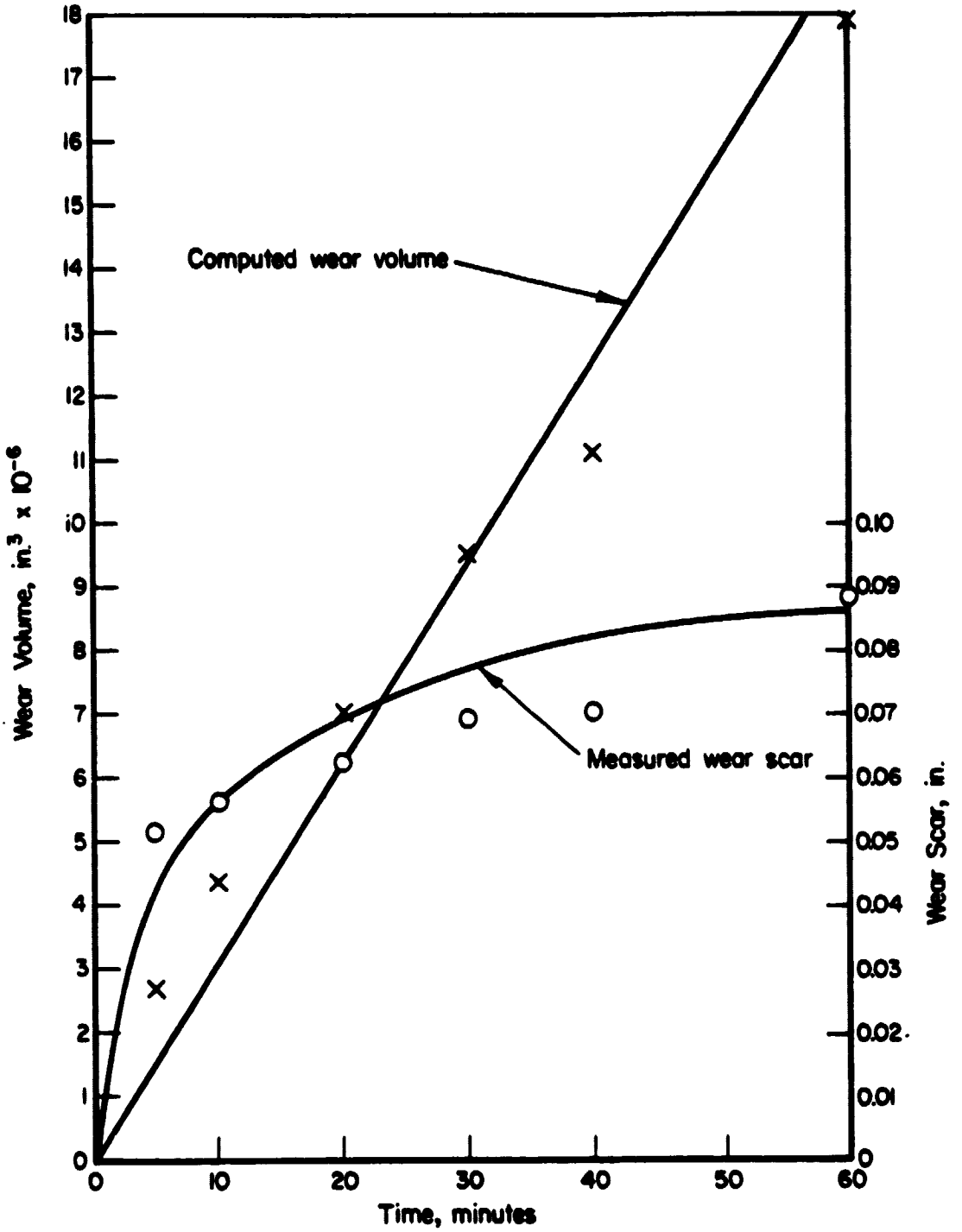

FIGURE 6. WEAR VOLUME AS A FUNCTION OF TIME FOR 440C UNCOATED BALL

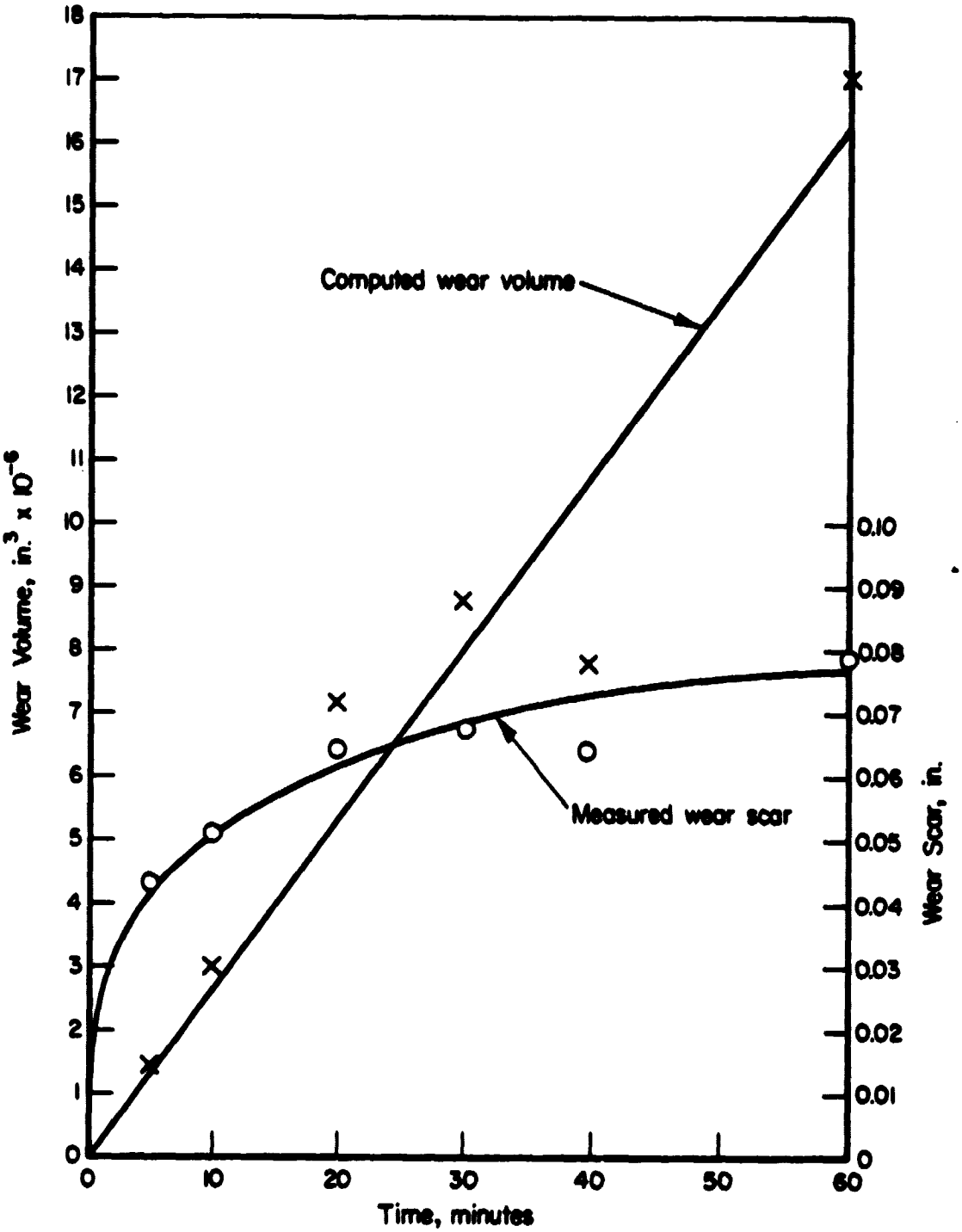

FIGURE 7. WEAR VOLUME AS A FUNCTION OF TIME FOR AISI 52100 STEEL BALLS

TABLE 5. SUMMARY OF 4-BALL WEAR TESTS UNDER AMBIENT CONDITIONS

Material	Coating Thickness (μm)	Environment	Friction Coefficient Initial	Friction Coefficient Final	Coating Duration Minutes	Wear Scar (mm,(in.)) (After 1 hour)
52100	-	Air	.57	.47	-	1.64 .0646
440C	-	Air	.57	.57	-	2.17 .0885
BG-42	-	Air	.43	.43	-	1.90 .0751
Star J	-	Air	.39	.39	-	3.58 .141
52100	1.5	Air	<.03	.49	13.	1.68 .066
440C	1.5	Air	<.03	.55	16.	1.68 .066
440C	.5	Air	<.03	.46	9.	1.75 .069
BG-42	1.5	Air	<.03	.61	45.	1.45 .057
BG-42	.5	Air	<.03	.57	6.	1.75 .06°
Star J	1.5	Air	<.03	.30	25.	3.18 .125
Star J	.5	Air	<.03	.46	20.5	3.71 .146

positioned around the 4-ball chamber (see Figure 2) which is, in turn, filled with LN_2. The level of LN_2 was monitored by two thermocouples; one was below the 4-ball contact zone and one was above the contact. In the experiments, the LN_2 flow was adjusted so that both thermocouples indicated the same temperature.

The results of the wear experiments for balls coated with MoS_2 operating at cyrogenic temperatures are summarized in Table 6. In general, the wear rates are quite consistent with the ambient wear rates. Typical values of the wear scar width range from .0109 to .0210 inch. Despite the similarity in wear rates, in general, the coating did not last as long at cryogenic temperatures. The longest coating life was 15 minutes for the Star-J material, although the average for the Star-J was 8.5 minutes for two experiments.

In general, the coated BG-42 and the 440C balls appear to be superior to the Star-J standard bearing material at cryogenic conditions. The test results can be averaged to yield the following rankings.

Material	Coating Life	Wear Scar (average)
BG-42	4 minutes	1.55 (.061)
440C	.75 minutes	1.52 (.060)
Star-J	8.5 minutes	2.87 (.113)

Test at Elevated Temperature

Although the SSME bearings operate in a cryogenic temperature environment, ball-race friction can result in severe hot-spots with the bearing. For this reason, some efforts have been given to the evaluation of the wear life and integrity of an MoS_2 film under high temperature (>400 F) conditions. For these experiments, the 4-ball test region was surrounded by an induction heating coil. The control thermocouple for the coil was located in the vicinity of the stationary three ball set. Temperatures well in excess of 800 F were possible with this arrangement.

TABLE 6. SUMMARY OF WEAR TEST UNDER LN_2 CONDITION

Material	Coating Thickness (μm)	Environment	Friction Coefficient Initial	Friction Coefficient Final	Coating Duration Minutes	Wear Scar (mm,(in.)) (After 1 hour)
440C	1.5	LN_2	<.03	.55	.5	1.50 (059)
440C	1.5	LN_2	<.03	.48	1.08	1.68 (066)
BG-42	1.5	LN_2	<.03	.63	4.0	1.83 (072)
BG-42	1.5	LN_2	<.03	.50	4.0	1.27 (050)
Star J	1.5	LN_2	<.03	.24	15.0	2.85 (.112)
Star J	1.5	LN_2	<.03	.38	2.0	2.92 (.115)
440C	PTFE	LN_2	<.03	.53	.5	1.50 (059)
440C	None	LN_2	<.03	.62	-	1.68 (066)
BG-42	None	LN_2	<.03	.53	-	1.50 (059)
Star J	None	LN_2	<.03	.34	-	2.00 (.079)

Ball wear and friction data at high temperatures are summarized in Table 7. It is obvious from these data that at a temperature of 204 C (400 F the coating can reduce friction somewhat, although at higher temperatures, severe wear occurs even with a coating on the surface.

TABLE 7. BALL FRICTION AND WEAR AT ELEVATED TEMPERATURES

Material	Coating Thickness (μm)	Temperature F°	Friction Coefficient Final	Wear Scar, mm(in.) (after 1 hour)
440C		400	.25	2.69 (.1060)
440C	1-1/2	400	.24	1.64 (.0645)
440C	1-1/2	800	.28	3.00 (.1181)
BG-42	1-1/2	400	.28	1.64 (.0644)
Star-J	1-1/2	400	.28	3.78 (.133)
Star-J	1-1/2	800	.28	3.30 (.130)

REFERENCES

1. Cheng, H., "Isothermal Elastohydrodynamic Theory for the Full Range of Pressure-Viscosity Coefficient", Trans. ASME, J. of Lub. Tech., Jan. 1972, pp 35-43.

2. Bell, J. C. and Kannel, J. W., "Interpretation of the Thickness of Lubricant Films in Rolling Contact II - Influence of Possible Rhelogical Factors", Trans. ASME, J. of Lub. Tech., Oct. 1971, pp 485-497.

3. Scott, R. B., Cyrogenic Engineering, D. Van Nostrand Co., NY, NY, 1959.

APPENDIX A

EVALUATION OF THERMAL EFFECTS IN CRYOGENIC EHD

APPENDIX A

EVALUATION OF THERMAL EFFECTS IN CRYOGENIC EHD

The objective of these analyses has been to develop equations for modeling the heat generation and temperature rise in the inlet region of a cryogenic EHD system. Also, state equations are presented which can be used to define whether the temperature has exceeded a critical level to maintain the cryogenic in a liquid state. The analyses are concerned only with the inlet region to the contact zone (see Figure A-1). This region has been found to be dominate in EHD film formation by numerous other researchers. The analyses incorporate the following lubrication theories.

1. Hertz (dry contact) theory for contact shape and dimension.
2. Equilibrium equation for lubrication.
3. Energy equation.
4. State equation for the fluid, including vapor pressure and viscosity.

Hertz (inlet) Shape Equation

The half width of contact can be expressed

$$b^2 = \frac{8\,WR}{\pi E} \quad p_o{}^2 = \frac{1}{2\pi}\,\frac{WE}{R} \quad \text{or} \quad b = 4\,R\,\beta_o \quad , \qquad \text{(A-1)}$$

where

b = half width of Herzian contact

p_o = maximum Hertz contact pressure

$\frac{1}{R} = \frac{1}{R_1} + \frac{1}{R_2}$ where $R_{1,2}$ are the radii of the surfaces

$\frac{1}{E} = \frac{1}{2}\left[\frac{1 - \nu_1{}^2}{E_1} + \frac{1 - \nu_2{}^2}{E_2}\right]$ where $E_{1,2}$ are Youngs modulii, ν is Poissons ratio

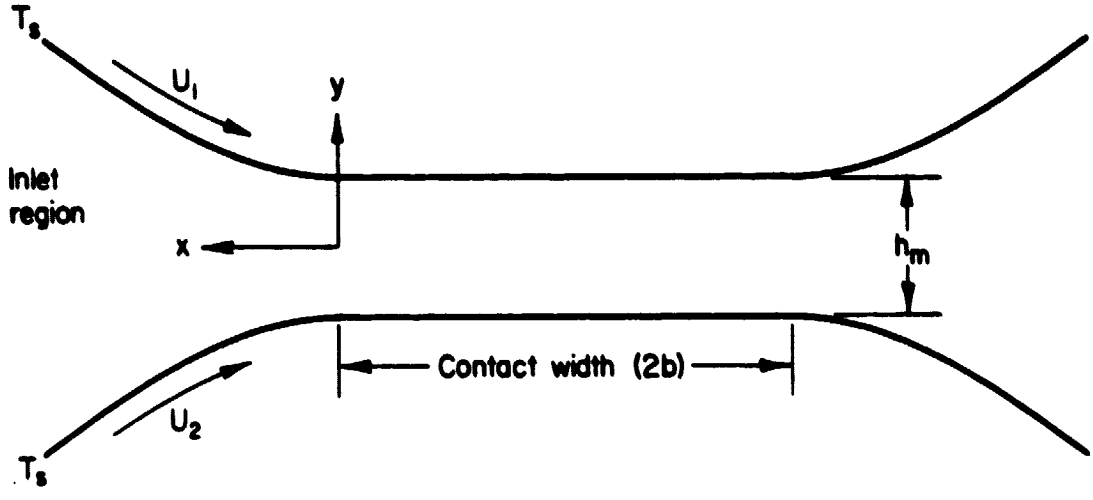

FIGURE A-1. NOMENCLATURE FOR ELASTOHYDRODYNAMIC FILM CALCULATIONS

w = load per unit width

$\bar{p}_o = p_o/E$

The shape of the inlet zone (see Figure A-1) can be written[2]

$$h = h_o + \frac{b^2}{2R} f\left(\frac{x}{a}\right) \quad , \tag{A-2}$$

$$\bar{h} = \bar{h}_o + 8\,\bar{p}_o^{\,2} f(\xi) \quad , \tag{A-3}$$

where

$$f(\xi) = (1 + \xi)\sqrt{\xi^2 + 2\xi} - \ln\left[1 + \xi + \sqrt{\xi^2 + 2\xi}\,\right] \quad , \tag{A-4}$$

here

$\bar{h} = h/R$

$\bar{h}_o = h_o/R$ (minimum film thickness)

$\xi = x/b$

Equilibrium Equation

The equilibrium equation for lubrication can be written

$$\frac{\partial}{\partial y}\left(\mu \frac{\partial u}{\partial y}\right) = \frac{\partial p}{\partial x} \quad , \tag{A-5}$$

where μ is lubricant viscosity and p is pressure. If we assume μ and p vary only with x, then

$$\frac{\partial \bar{p}}{\partial \bar{x}} = 4\left[\frac{\mu\, U\, \bar{p}_o}{RE\, \bar{h}^2}\right] \frac{\partial^2 \bar{u}}{\partial\, \bar{y}^2} \quad . \tag{A-6}$$

Also, Equation (A-6) can be solved to yield the familiar Reynolds equation

$$\frac{\partial \bar{p}}{\partial \bar{x}} = 48\left[\frac{\mu\, U\, \bar{p}_o}{RE}\right] \frac{\bar{h} - \bar{h}_o}{\bar{h}^3} \quad , \tag{A-7}$$

where

μ is the lubricant viscosity

U is the average velocity of the surface $1/2(U_1 + U_2)$

$\bar{p}$ = pressure divided by E

$\bar{y}$ = y/h.

Energy Equation

If we assume the primary source of heat transfer is conduction from (or to) the lubrication film and convection along the film, the energy equation can be written

$$K \frac{\partial^2 T}{\partial y^2} = \mu \left(\frac{\partial u}{\partial y}\right)^2 + \rho c \frac{\partial T}{\partial t} \quad , \tag{A-8}$$

or

$$\underbrace{\frac{T_s K}{R^2 \bar{h}^2} \frac{\partial^2 \bar{T}}{\partial \bar{y}^2}}_{\text{conduction}} = \underbrace{-\left(\frac{\mu U^2}{R^2 \bar{h}^2}\right)\left(\frac{\partial \bar{u}}{\partial \bar{y}}\right)^2}_{\text{generation}} + \underbrace{\left(\frac{\rho C T_s U}{4R \bar{p}_o}\right)\frac{\partial \bar{T}}{\partial \bar{t}}}_{\text{convection}} \quad , \tag{A-9}$$

where T is temperature, T_s is the surface temperature in the bearing and t and $\bar{T} = T/T_s$ and t is the time a lubrication element is in the inlet region, ($t = x/u$ and $\bar{t} = U/b\ t$).

State Equations

The viscosity for lubricants in EHD contacts is normally written

$$\frac{\mu}{\mu_o} = \exp\left[(\gamma E)\ \bar{p} - (\alpha T_s)\ \bar{T}\right] \quad . \tag{A-10}$$

Where, for a cryogenic fluid, it is possible that at some point, the temperature rise will cause the fluid to be above its vapor pressure. At this point, the fluid could become gaseous and lose its liquid viscosity. Vapor pressure data for liquid oxygen and liquid hydrogen are given in reference 3, (pp 274 and 298). These data were modeled by the following equations

for oxygen

$$T = 2.16 \left[\ln \frac{p}{.105}\right]^2 + 108 \quad \text{(degrees R)} \quad , \qquad \text{(A-11)}$$

for hydrogen

$$T = .708 \left[\ln \frac{p}{.109}\right]^2 + 19.8 \quad \text{(degrees R)} \quad , \qquad \text{(A-12)}$$

where p is in psia ($p > .109$).

The heat of vaporization for oxygen can be approximated by

$$\begin{aligned} Q_{vap} &= 18.4\ (280 - T)^{.33} \quad \text{(BTU/lb)} \\ Q_{vap} &= 6.2 \times 10^3\ (280 - T)^{.33} \quad \text{(in.-lb/in.}^3\text{)} \end{aligned} \quad , \qquad \text{(A-13)}$$

where T is in degrees Rankine $T < 280$.

Temperature Solution

The purpose of the analyses is to determine average temperature and heat generation at any x-position along the inlet zone. The temperature solutions for any such x-position involve solving Equation (A-9) in conjunction with Equations (A-6) and (A-7). For these analyses, it will be assumed that both surfaces are at the same temperature and are moving at the same speed. With these assumptions, Equation (A-6) can be integrated to show

$$\frac{\partial \bar{p}}{\partial \bar{x}}\,\bar{y} = 4\left[\frac{\mu\, U \bar{\beta}_0}{R_E\, \bar{h}^2}\right] \frac{\partial \bar{u}}{\partial \bar{y}} \quad . \qquad \text{(A-14)}$$

Combining Equation (A-14) with Equation (A-7) shows

$$\frac{\partial \bar{u}}{\partial \bar{y}} = 12\,\frac{\bar{h} - \bar{h}_0}{\bar{h}}\,\bar{y} \quad . \qquad \text{(A-15)}$$

The average heat generation across the film (first term on left side of Equation (A-9)) can be written

$$\text{ave} = 12\left(\frac{\mu\, U^2}{R^2}\right)\frac{(\bar{h} - \bar{h}_0)^2}{\bar{h}^4} \quad . \qquad \text{(A-16)}$$

If

$$\bar{t} = \frac{4R\bar{p}_o\bar{x}}{U} \qquad ot = \frac{4Rp_o}{U}\int_0^{\bar{x}} Q_{ave}\, d\,\bar{x}' \quad . \tag{A-17}$$

Equation (A-14) could be used in conjunction with Equation (A-9) to express the temperature of the fluid in the inlet zone. However, Equation (A-9) is extremely difficult to solve for inlet zone equations. This difficult occurs as the result of $\bar{h}$ being x dependent and from the variation in both magnitude and direction of the fluid motion u. If we ignore convection and combine Equations (A-7), (A-15), and (A-9), there results

$$\frac{\partial^2\bar{T}}{\partial\bar{y}^2} = -144\left[\frac{\mu U^2}{KT_s}\right]\frac{(\bar{h}-\bar{h}_o)^2}{\bar{h}^2}\,\bar{y}^2 \quad . \tag{A-18}$$

Equation (A-18) can be readily solved for T as follows

$$\bar{T} = .75\left[\frac{\mu U^2}{KT_s}\right]\frac{(\bar{h}-\bar{h}_o)^2}{\bar{h}^2}\left[1 - 16\,\bar{y}^4\right] + 1 \quad . \tag{A-19}$$

The average temperature is given by

$$\bar{T}_{ave} = .75\left[\frac{\mu U^2}{KT_s}\right]\frac{(\bar{h}-\bar{h}_o)^2}{\bar{h}^2} + 1 \quad . \tag{A-20}$$

Calculating Units

Since the bearing drawing and all input data provided by NASA were in English units, all calculations were performed in English units. Therefore, the SI units presented in this report were converted from English units. The data on which this report is based is located in Battelle Laboratory Record Boon Number 34405.